

# A New Car-Following Model Inspired by Galton Board

Fa Wang, Li Li, Xuexiang Jin, Jianming Hu, Yi Zhang, Yan Ji\*

(Dated: July 19, 2008)

## Abstract

Different from previous models based on scatter theory and random matrix theory, a new interpretation of the observed log-normal type time-headway distribution of vehicles is presented in this paper. Inspired by the well known Galton Board, this model views driver's velocity adjusting process similar to the dynamics of a particle falling down a board and being deviated at decision points. A new car-following model based on this idea is proposed to reproduce the observed traffic flow phenomena. The agreement between the empirical observations and the simulation results suggests the soundness of this new approach.

PACS numbers: 45.70.Vn, 89.40.-a, 02.50.-r,

---

\*Department of Automation, Tsinghua University, Beijing 100084, P. R. China; Electronic address: li-li@mail.tsinghua.edu.cn

## I. INTRODUCTION

To explain and reproduce the complex phenomena of road traffic, the dynamics of traffic flows are often described on  $N$  strongly-linked particles (vehicles) under fluctuations [1], [2], [3]. Since the governing interaction forces or potentials cannot be directly measured, the statistical distributions of particles are often investigated instead [4], [5].

Among different statistical features, the distributions of space-gaps/time-headways between these particles (vehicles) received consistent interests from various viewpoints. In transportation engineering, the corresponding investigation data are helpful not only in understanding the microscopic-level driving behaviors but also in estimating the macroscopic-level roadway capacities [6], [7], [8], [9]. Numerous distribution models have been developed over the past 50 years to directly fit the empirical data. In some recent studies [11], [12], [13], [14], some theoretical models were presented from various physical perspectives (e.g. scatter theory and random matrix theory) to explain why we can observe similar distributions even for different phases (i.e. Kerner's the free-flow, synchronized flow, and moving jam phases [4]).

Differently in this paper, another interpretation inspired by the well-known Galton board is presented. A new car-following model based on this interpretation is also proposed to reproduce the observed traffic flow phenomena. The research purposes are twofold here: 1) Previous physical interpretations focus on the steady-state macroscopic-level statistics; while this method provides a microscopic-level dynamic explanation, which can also be used to simulation the transient-state statistics of inter-arrival and inter-departure vehicle queuing interactions. 2) It is interesting that as a slightly modified extension of the classic car-following model, this new model can easily reproduce the observed time-headway distributions, which had been neglected by many previous approaches.

## II. THE LOG-NORMAL DISTRIBUTION MODEL OF TIME-HEADWAYS

Based on several recent studies [5], [9], [10], [11], [14], we believe that log-normal distribution model is a simple yet effective model comparing to other ones, i.e. distribution models according to random-matrix theory [5], [14]. For example, Fig. 1 shows the comparison results for the empirical, super-statistical on random matrix theory [14] and log-normal

distributions  $P(\tau)$ , where  $\tau = t_h/\langle t_h \rangle$ ,  $t_h$  denotes the sampled time headways. It is clear that log-normal distribution model leads to smaller fitting errors.

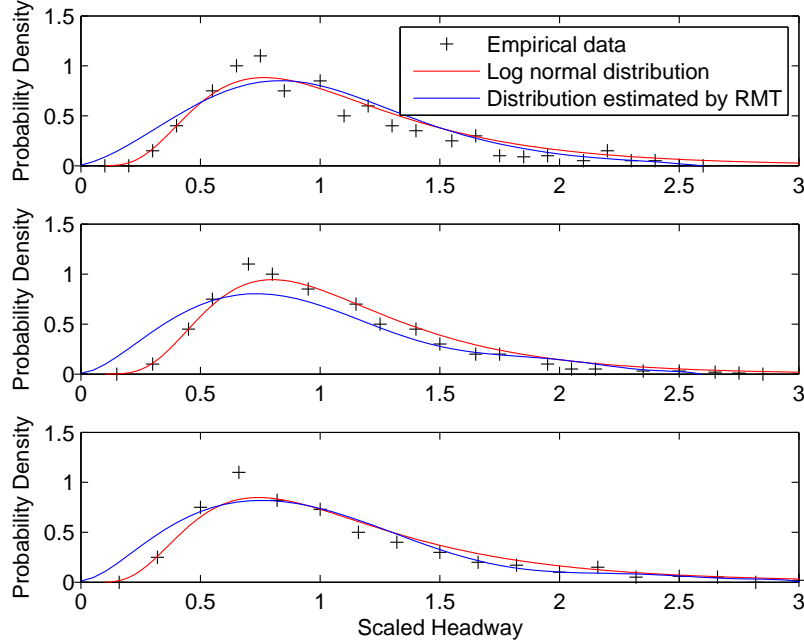


FIG. 1: Probability density  $P(\tau)$  for scaled empirical time headways  $\tau$  between successive cars in traffic flow. For comparison, the empirical data and super-statistical distributions on random matrix theory are excerpted from [5].

Moreover, log-normal distribution model can also be used to depict the distributions of time headways in transient-state flow. For instance, the departure headways (which are usually defined as the times that elapse between consecutive vehicles when vehicles in a queue start crossing the stop line) are shown to follow log-normal distributions in [19].

Noticing that the random matrix theory gives a soundable explanation for its corresponding distribution model, an interesting question naturally arises as: “Can we provide a physical interpretation of such log-normal distributions?” After comparing with the other dynamic processes that yield log-normal distribution [15], [16], [17], [18], we think the outcomes of such distributions can be explained as follows.

In car-following process, the driver of the following vehicle will adjust his/her velocity from time to time to track the leading vehicle and meanwhile keep a safe distance between the leading vehicle and him/her. Because the leading vehicle’s movement is often unpredictable

(at least not fully predictable), the accelerating and braking action of the driver is often overdue.

This persistent velocity adjusting process is somewhat like the process of the particles falling down a board and being deviated at decision points (the tips of the triangular obstacles) either left or right with equal probability, see Fig. 2. If the deviation of the particle from one row to the next is a random additive process with possible values  $+c$  and  $-c$ , the normal distribution will be created by the board, which reflects the cumulative additive effects of the sequence of decision points. But if the deviation of the particle from one row to the next is a random multiplicative process with possible values  $\cdot c'$  and  $/c'$ , the log-normal distribution will be generated.

It is obvious that drivers tend to take very careful acceleration when the spacing between the two vehicles is small and do not want to speed up at once after braking. Thus, the deviation of the particle to the left is equivalent to the following vehicle's accelerating action, since the relative speed decrease slowly at this period; while the deviation to the right is equivalent to the following vehicle's braking action, since the relative speed increase quickly at this period. From this view point, the car-following process is similar to the particles falling in the log-normal type Galton board. To verify this conjecture, a microscopic simulation model inspired by log-normal type Galton board is proposed in the next section to reproduce the observed phenomena.

### III. THE NEW CAR-FOLLOWING MODEL INSPIRED BY GALTON BOARD

In this section, it will be interesting to find that a car-following model incorporating Galton Board mechanism can be easily derived from a famous classic car-following model proposed in later 1950s [20], [21]. The proposed model mainly depicts three states of a vehicle: 1) stopped, 2) starting-up, and 3) driving/braking states. More precisely, they can be described as follows.

Suppose  $v_i(t)$  and  $x_i(t)$  are the velocity and position of the  $i$ th vehicle (follower) at time  $t$ , respectively. Similarly,  $v_{i-1}(t)$  and  $x_{i-1}(t)$  are the velocity and position of the  $i - 1$ th vehicle (leader) at time  $t$ .  $g_i(t) = x_i(t) - x_{i-1}(t) - l_i$  denotes the gap between the two vehicles at time  $t$ .  $T \geq 0$  is the simulation time span.

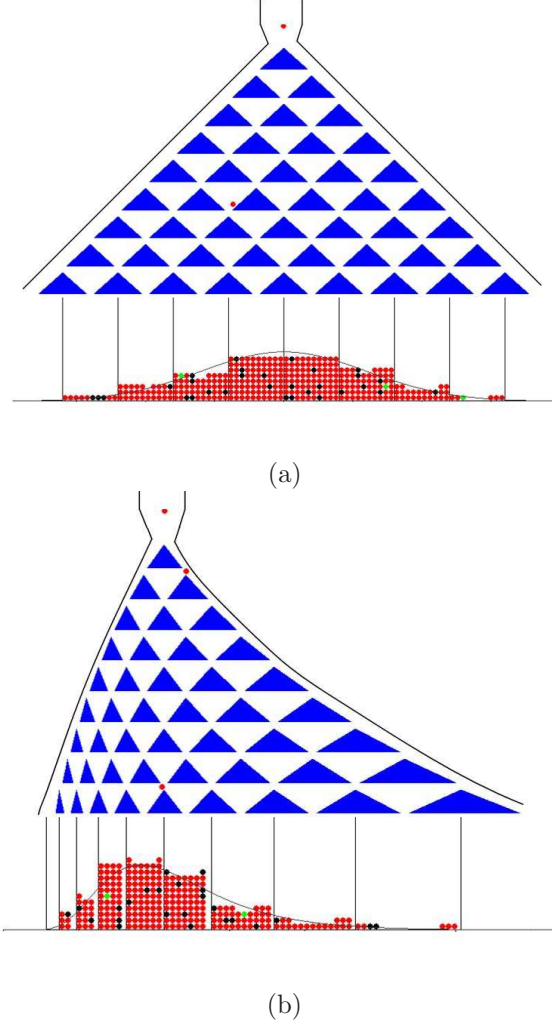


FIG. 2: Diagram of two Galton boards yielding normal (a) and log-normal (b) distributions respectively. If the tip of a triangle is at distance  $x$  from the left edge of the board, triangle tips to the right and to the left below it are placed at  $x + c$  and  $x - c$  for the normal distribution, and  $x \cdot c'$  and  $x/c'$  for the log-normal, where  $c$  and  $c'$  are constants.

1) If  $v_i(t) = 0$ , that is, the  $i$ th vehicle is fully stopped at time  $t$ ; it will stay stopped in the next time interval  $T$  and then enter the starting state since time  $(t + T)$ .

2) Else if the  $i$ th vehicle is in the starting-up state at time  $t$ , it will check its coming actions from the following three choices:

2.a) If  $g_i(t) < G_{min}$ , where  $G_{min}$  is the minimum stop distance. The  $i$ th vehicle will go back to stop state by letting  $v_i(t + T) = 0$  without doing anything else (that's,  $x_i(t + T) = x_i(t)$ ).

2.b) Else if  $v_i(t) < v_{starting}$ , where  $v_{starting}$  is the limit of the starting-up velocity; the

vehicle is still in the starting-up state at time  $(t + T)$ . Thus, it will accelerate with the starting-up rate  $a_{starting}$  in the next time interval  $T$  till time  $(t + T)$ .

2.c) Otherwise, the vehicle will switch to the driving/braking state since time  $t$  and re-determine its action according to the updating rules set for the driving/braking state at time  $t$ .

3) Otherwise, the vehicle is running in the driving/braking state. Actually, the driving/braking state contains three modes: 3.a) free-driving mode, 3.b) braking model and 3.c) following mode (see Fig. 3), which can be represented in details as:

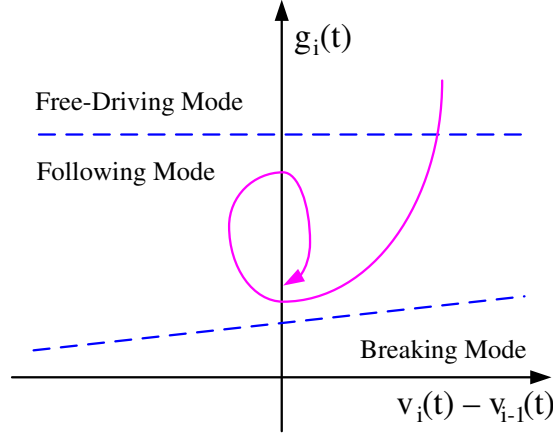


FIG. 3: Diagram of the three modes (regions) in the gap vs. relative-speed space. Comparing to Fritzsche 1994 model used in PARAMICS and Wiedemann Psychophysical model used in VISSIM, our model has fewer modes.

3.a) If  $g_i(t) > G_{max}$ , where  $G_{max}$  is the maximum coupling distance; the  $i$ th vehicle is in free-driving mode. It will try to approach the highest velocity as

$$v_i(t + T) = \min\{v_i(t) + a_{max}^+ \times T, v_{max}\} \quad (1)$$

where  $a_{max}$  is the maximum allowable acceleration rate. For simplicity, we choose  $T = 1$  second here.

3.b) Else if  $v_i(t) - v_{i-1}(t) > [g_i(t) - G]/H$ , there exists a risk to collide, and  $i$ th vehicle is in braking mode. It will try to stop as quickly as possible

$$v_i(t + T) = v_i(t) - D \times T \quad (2)$$

where  $G$ ,  $H$  and  $D$  are positive constants denoting the minimum safety gap, deceleration time and braking decelerating rate, respectively.

3.c) Otherwise, the  $i$ th vehicle is in the following mode. We have the following two-step updating rules as

$$\tilde{v}_i(t+T) = \begin{cases} \max\{\beta v_i(t) \frac{x_i(t)-x_{i-1}(t)-l_i}{x_i(t-T)-x_{i-1}(t-T)-l_i}, 0\}, & \text{with probability } p \text{ to decelerate} \\ \min\{\frac{1}{\beta} v_i(t) \frac{x_i(t)-x_{i-1}(t)-l_i}{x_i(t-T)-x_{i-1}(t-T)-l_i}, v_{max}\}, & \text{with probability } (1-p) \text{ to accelerate} \end{cases} \quad (3)$$

$$v_i(t+T) = \begin{cases} \max\{\tilde{v}_i(t), v_{i-1}(t) - a_{max}^- \times T\}, & \text{if decelerate} \\ \min\{\tilde{v}_i(t), v_{i-1}(t) + a_{max}^+ \times T\}, & \text{if accelerate} \end{cases} \quad (4)$$

where  $l_i$  denotes the length of the  $i$ th vehicle.  $v_{max}$  is the maximum allowable velocity.  $a_{max}^+$  and  $a_{max}^-$  are the maximum allowable car-following ac/deceleration rates. The max, min functions are added to guarantee that the velocity and ac/decelerating rates are within the limits.  $\beta$  is a positive constant to be determined according to investigation data.

Eq.(3)-(4) characterize the simulated time headways to follow the log-normal distributions. A brief explanation of this mechanism is provided in the Appendix. It is assumed that  $0 < \beta \lesssim 1$  together with  $0 < p < 0.5$ , since drivers tend to keep a close spacing. We can see that Eq.(3)-(4) naturally incorporate the frequently-used randomly-slow-down features of driving behaviors.

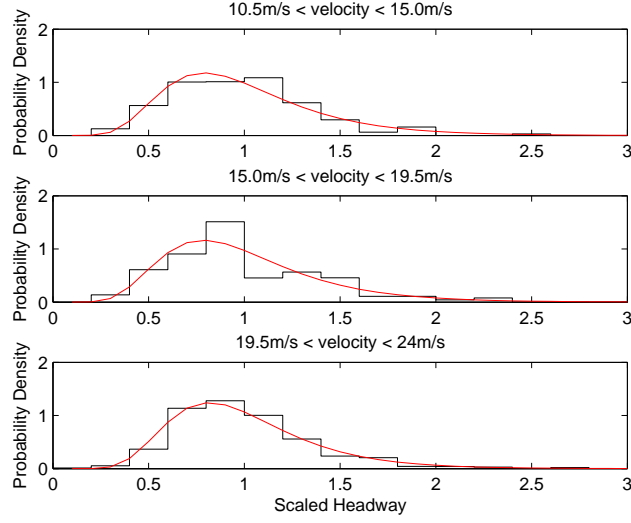
4) Finally, the position of vehicle is updated as

$$x_i(t+T) = x_i(t) + v_i(t+T) \times T \quad (5)$$

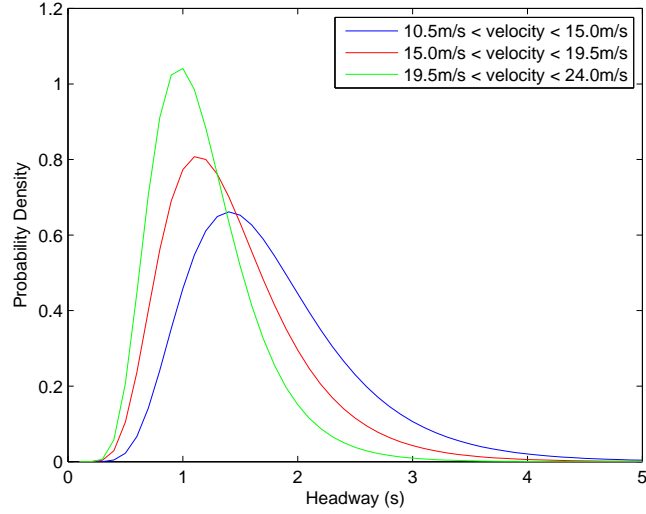
To illustrate the effectiveness of the proposed model, a specialized form is used to reproduce the complex phenomena of freeway traffic flows. Particularly, we have all the vehicles have the same length as  $l_i = 4\text{m}$  and  $T = 1\text{s}$ . Other parameters are set as  $v_{starting} = 8\text{m/s}$ ,  $a_{starting} = 4\text{m/s}^2$ ,  $G_{min} = 0.5\text{m}$ ,  $G_{max} = 52.5\text{m}$ ,  $v_{max} = 30\text{m/s}$ ,  $a_{max}^+ = 4\text{m/s}$ ,  $a_{max}^- = 8\text{m/s}$ ,  $\beta = 0.93$ ,  $p = 0.3$ .  $G = 0.5\text{m}$ ,  $H = 7\text{s}$ ,  $D = 8\text{m/s}^2$ .

Fig. 4 shows the corresponding distributions of the simulated time headways within different velocity ranges. The log-normal distribution model passes the Kolmogorov-Smirnov

(K-S)hypothesis test. This proves that the new model yields the log-normal type time-headway distribution as observed; while many previous models yield symmetric distributions, i.e. Fig. 7 of [23]. Moreover, as the velocity of the vehicle increases, the mean time headways of such log-normal type distributions will approach the saturation headway. This fits the observations [5], [24], too.



(a)



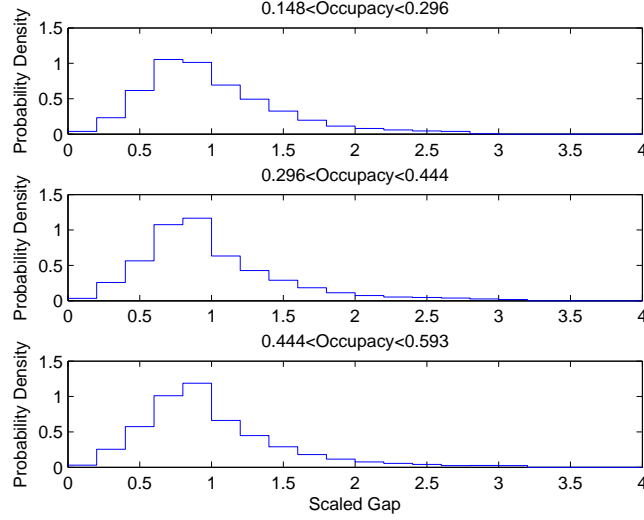
(b)

FIG. 4: Probability density for (a) scaled simulated time headways  $\tau$  and (b) un-scaled simulated time headways  $t_h$  between successive cars in traffic flow.

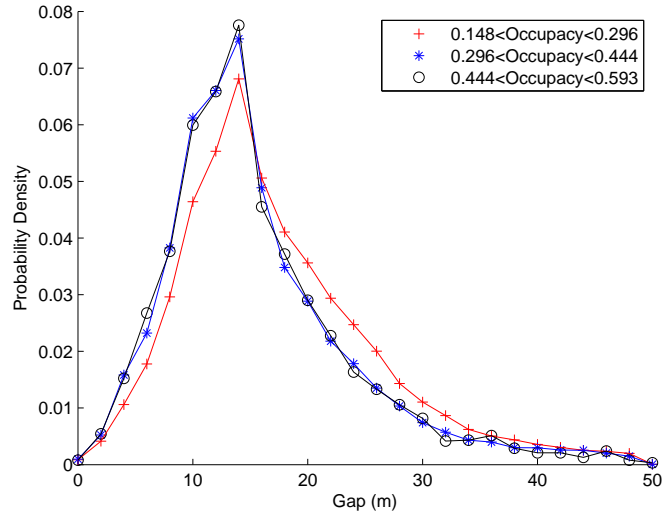
Fig. 5 shows the corresponding distributions of the simulated space gaps under different



traffic pressures. As the traffic flow density (occupancy) increases, the distribution of space gaps will become more concentrated, which is in accordance with the practical observations (see the un-scaled distributions shown in Fig. 3a in [13] for comparison). Moreover, the shape of the un-scaled simulated gap distributions look similar to the empirical data and also the scaled distributions predicted by using random matrix theory (see that shown in Fig. 1 in [14] for comparison).



(a)



(b)

FIG. 5: Probability density for (a) scaled simulated space gaps  $\iota = g_s / \langle g_s \rangle$  and (b) un-scaled simulated space gaps  $g_s$  between successive cars in traffic flow.

Fig. 6 show the  $(k, \bar{v}_s)$  and  $(k, q)$  diagrams for the proposed model, obtained by local and global measurements. These macroscopic traffic stream characteristics are measured according to [22]. Here,  $K_g$  denotes the length of the closed single-lane system, which is 27000m. It can be found that the local measurements in Fig. 6 also discriminate Kerner's three-phase flows: the free-flow regime contains only a few data points on a line; the synchronized regime is formulated by widely scatters of the data points; and jammed regimes contains the data points corresponding to Kerner's line  $J$ .

Fig. 7 shows three typical complex phenomena reproduced by using the proposed model: (a) the oscillation in traffic flow; (b) the wide moving jam; and (c) the stop-and-go waves. This proves that the proposed model is capable to describe the other complex dynamic features of road traffic flow, too.

## APPENDIX: EXPLANATION OF THE LOG-NORMALITY

According to the Galton board model, if the variation dynamics of time headway should be depicted by the following equation without losing any generality.

$$t_h(t) = \begin{cases} \beta t_h(t-T), & \text{with probability } (1-p) \\ \frac{1}{\beta} t_h(t-T), & \text{with probability } p \end{cases} \quad (\text{A.1})$$

Notice that be definition, we roughly have

$$t_h(t) \approx \frac{g_s(t)}{v(t+T)} \quad (\text{A.2})$$

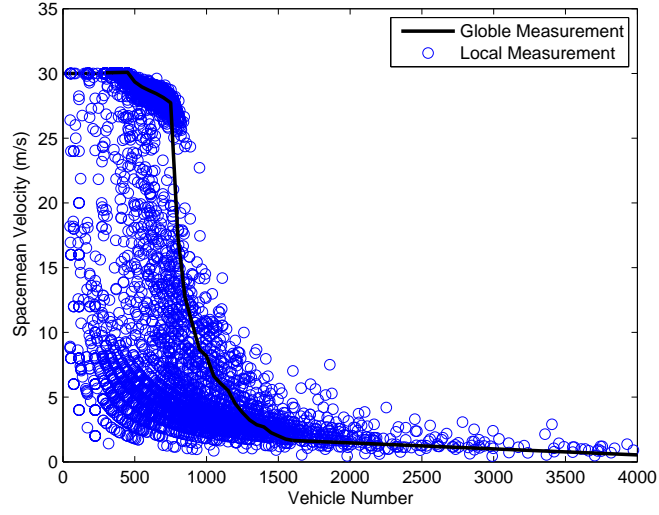
we can then have

$$\frac{g_s(t)}{v(t+T)} = \begin{cases} \beta \frac{g_s(t-T)}{v(t)}, & \text{with probability } (1-p) \\ \frac{1}{\beta} \frac{g_s(t-T)}{v(t)}, & \text{with probability } p \end{cases} \quad (\text{A.3})$$

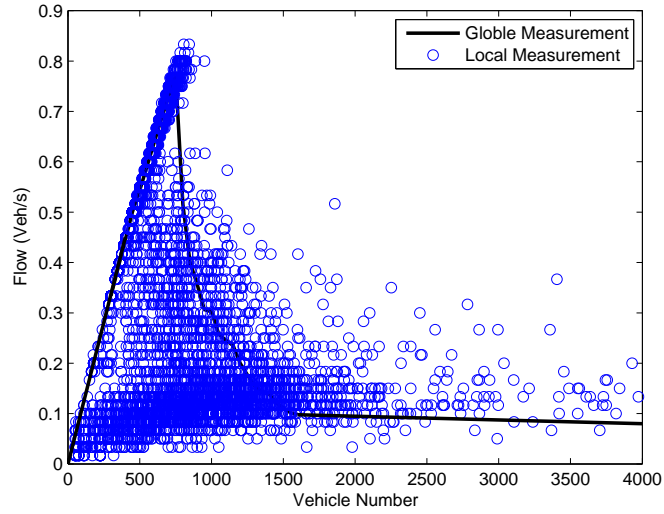
Considering the pre-determined limits of the velocity and ac/deceleration rates, we can directly derive Eq.(4) from Eq.(A.3) then.

## ACKNOWLEDGMENTS

This work was supported in part by National Basic Research Program of China (973 Project) 2006CB705506, Hi-Tech Research and Development Program of China (863



(a)



(b)

FIG. 6: (a) The  $(k, \bar{v}_s)$  diagram for the proposed model, obtained by local and global measurements.

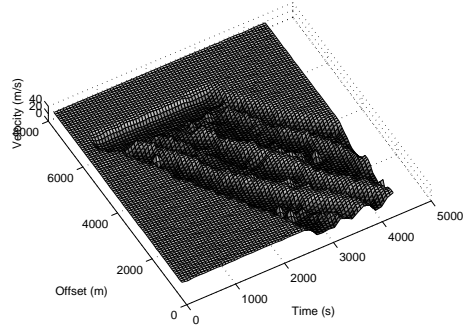
(b) The  $(k, q)$  diagram for the proposed model, obtained by local and global measurements.

Project) 2006AA11Z208, 2006AA11Z229 2007AA11Z222, and National Natural Science Foundation of China 50708055.

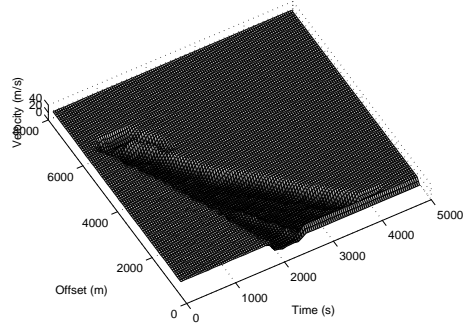
---

[1] D. Chowdhury, L. Santen, A. Schadschneider, *Phys. Rep.* **329**, 199 (2000).

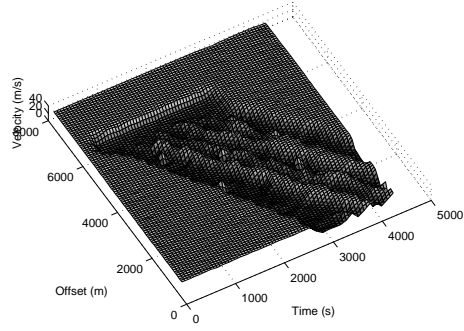
[2] D. Helbing, *Rev. Mod. Phys.* **73**, 1067 (2001).



(a)



(b)



(c)

FIG. 7: The spatiotemporal speed diagrams of: (a) the oscillation in traffic flow; (b) the wide moving jam; and (c) the stop-and-go waves.

[3] R. Mahnke, J. Kaupuzs, I. Lubashevsky, *Phys. Rep.* **408**, 1 (2005).

[4] B. S. Kerner, *The Physics of Traffic* (Springer, Heidelberg, 2004).

[5] B. S. Kerner, S. L. Klenov, A. Hiller, and H. Rehborn, *Phys. Rev. E* **73**, 046107 (2006).

[6] R. T. Luttinen, *Transp. Res. Rec.* **1365**, 92 (1992).

- [7] P. G. Michael, F. C. Leeming, W. O. Dwyer, *Transp. Res. F*, **3**, 55 (2000).
- [8] *Highway Capacity Manual*, (The Transportation Research Boards, National Research Council, Washington, DC, 2000).
- [9] G. Zhang, Y. Wang, H. Wei, Y. Chen, *Traffic Flow Theory 2007*, 141 (2007).
- [10] C. Thiemann, M. Treiber, A. Kesting, arXiv:0804.0108
- [11] M. Krbalek, P. Seba, P. Wagner, *Phys. Rev. E* **64**, 066119 (2001).
- [12] M. Krbalek, D. Helbing, *Physica A* **333**, 370 (2004).
- [13] D. Helbing, M. Treiber, A. Kesting, *Physica A* **36**, 62 (2006).
- [14] A. Y. Abul-Magd, *Phys. Rev. E* **76**, 057101 (2007).
- [15] F. Galton, *Natural Inheritance*, (Macmillan, London, 1889).
- [16] J. Aitchison, J. A. C. Brown, *The Lognormal Distribution*, (Cambridge University Press, Cambridge, 1957).
- [17] E. L. Crow, K. Shimizu, eds. *Lognormal Distributions: Theory and Application*, (Dekker, New York, 1988).
- [18] E. Limpert, W. A. Stahel, M. Abbt, *Bioscience* **51**, 341 (2001).
- [19] Y. Su, Z. Wei, S. Cheng, D. Yao, Y. Zhang, L. Li, Z. Zhang, Z. Li, in *Transportation Research Board Annual Meeting CD*, (2008).
- [20] D. C. Gazis, R. Herman, R. B. Potts, *Operations Research* **7**, 499 (1959).
- [21] N. H. Gartner, C. J. Messer, A. K. Rathi, *Revised Monograph on Traffic Flow Theory*, (Transportation Research Board, 1997).
- [22] S. Maerivoet, B. De Moor, *Phys. Rep.* **419** (2005) 1.
- [23] M. Bando, K. Hasebe, A. Nakayama, A. Shibata, Y. Sugiyama, *Phys. Rev. E*, **51** (1995) 1035.
- [24] M. Schonhof, D. Helbing, *Transp. Sci.* **41**, 135 (2007).